CHEMISTRY
A EUROPEAN JOURNAL

DOI: 10.1002/chem.200500909

Bond Orders between Molecular Fragments

Adam J. Bridgeman* and Christopher J. Empson[a]

Abstract: An extension of the Mayer bond order for the interaction between molecular fragments is presented. This approach allows the classical chemical concepts of bond order and valence to be utilised for fragments and the interactions between the fragments and symmetry-adapted linear combinations to be analysed. For high-symmetry systems, the approach allows the contribution from each irreducible representation to be assessed and provides a semiquantitative measure of the role of each bonding mode to interfragment interactions. The utility of this tool has been examined by a study of the bonding in symmetrical sandwich complexes. The validity of the frontier-orbital approach and the contributions from each frontier-orbital interaction can also be assessed within this model. As demonstrated by a study of a number of mixed-sandwich complexes, the model proves to be especially useful for low-symmetry systems in which separation of the σ, π and δ roles in bonding of the ligand is difficult to assess. The fragment bond order describes the interaction between preoptimized fragment orbitals and is independent of the charges that are placed on these fragments. Although the method allows the chemist to define fragments in any way they choose, most insight is gained by using the same frontier orbitals employed so successfully in perturbational molecular-orbital approaches. The results are free from the influence of the electron-counting method used to describe fragments, such as the rings and metals in sandwich complexes.

Keywords: bond theory · cyclopentadienyl ligands · density functional calculations · main group elements · transition metals

Introduction

Bond multiplicity, atomic charge and valency are key concepts in the way in which the covalent and electrostatic interactions between atoms and the chemical characteristics and identities of elements are described. These terms form the language that we use to portray the formation of molecules and the building of chemical structures from atoms. Despite the utility of these notions in teaching and describing chemistry, no quantum-mechanical operators have been derived to calculate them. In electronic-structure methods, molecular orbitals (MOs) are commonly constructed from linear combinations of atomic orbitals so that analysis also focuses on atomic and diatomic terms through the calculation of partial charges and bond orders. The "atoms in molecules" (AIM) approach developed by Bader[1] has shown that molecules can be partitioned into atoms and that terms such as chemical bonds and atomic quantities, including charge, volume and energy, emerge through a topological analysis of the electron density.

The influence of Lewis structures and, in particular, the concept of sharing of electron pairs between atoms in molecules is very strong, although their connection with the MOs or electron density generated by modern quantum-chemical methods is not at all obvious. It is known that MOs can, in many cases, be transformed into localized orbitals, which reflect the diatomic nature of bonding implicit in chemical structures. Analysis based on the delocalized orbitals, however, is often more transparent when discussing reactivity, when comparing related systems and when showing the connections between apparently unrelated systems. Delocalized orbitals also reflect the symmetry of molecules allowing the power of symmetry theory to be applied in both their construction and analysis.[2,3] Diatomic or even multicentred bond orders and atomic charges can be calculated from delocalized orbitals to generate local information about bonding. Classically, the bond multiplicity reflects the number of

[a] Dr. A. J. Bridgeman, C. J. Empson
Department of Chemistry, University of Hull
Kingston-upon-Hull, HU6 7RX (UK)
Fax: (+44) 1482-465464
E-mail: a.j.bridgeman@hull.ac.uk

Supporting information for this article is available on the WWW under http://www.chemeurj.org/ or from the author. Supporting Information Available: A comparison of optimized and experimentally determined bond lengths for the sandwich complexes $[M(\eta^5\text{-}C_5H_5)_2]$ (M = Mg, Ca, Sr, Ba, and Fe), $[Cr(\eta^6\text{-}C_6H_6)_2]$ and $[M(\eta^5\text{-}C_5H_5)(\eta^x\text{-}C_xH_x)]$ (M = Cr; $x = 7$, M = Mn; $x = 6$, M = Co; $x = 4$, M = Ni; $x = 3$).

shared electron pairs between atoms; various models have been proposed for its analogue in the MO method. A number of definitions of bond order have been proposed based on the density matrix formed from the atomic coefficients of the occupied MOs.[4] The definition which we have found particularly valuable in analyses of inorganic molecules[4] and clusters[5,6] is that due to Mayer.[7] The Mayer bond order, β_{AB}, between two atoms, A and B, in a closed-shell molecule is given by Equation (1), in which **P** and **S** are the density and overlap matrices; the summations run over the atomic orbitals (AOs) centred on the two atoms.

$$\beta_{AB}(AO) = \sum_{i}^{\text{on A}} \sum_{j}^{\text{on B}} (\mathbf{PS})_{ij}(\mathbf{PS})_{ji} \quad (1)$$

For simple, homonuclear diatomics, the Mayer bond order is equal to the classical bond multiplicity, at least for minimal basis sets. The Mayer bond order, itself a generalization of the Wiberg[8] bond order widely used in zero-overlap theories, is applicable to any single-determinant techniques including various semiempirical, Hartree–Fock and density-functional methods. Bond orders are particularly valuable for large and low-symmetry molecules, in which the interactions between pairs of atoms may be distributed over many occupied levels. For many high-symmetry systems, we have shown previously,[4] and exploited for a variety of systems,[4–6] that the Mayer bond order can be expressed as a sum over symmetry species Γ [Eq. (2)].

$$\beta_{AB}(AO) = \sum_{\Gamma} \beta^{\Gamma}_{AB}(AO) \quad (2)$$

This decomposition allows calculation of the separate σ and π contributions to bonds, either by use of the full molecular point group or by lowering the symmetry to resolve the contributions from degenerate orbitals. A typical use of the diatomic bond order would be the calculation of the σ and π contributions to the Cr–C bond order in any molecule containing a Cr–CO bond. As the summation in Equation (1) is over pairs of atomic orbitals, the relative importance of the chromium 3d, 4s and 4p orbitals can also be assessed.

The covalency of an atom, C_A, can be simply written as a sum of all of the bond orders made by the atom. The Mayer prescription for the bond order is closely related to that proposed by Mulliken for the atomic partial charge, Q_A, allowing a definition of the total "bonding power" or valency of an atom in a molecule[9] as a combined measure of covalent (covalency) and ionic (electrovalent) bonding [Eq. (3)].

$$V_A = \frac{1}{2}[C_A + (C_A{}^2 + 4Q_A{}^2)^{1/2}] \quad (3)$$

We have shown previously, for example, that the valency of oxygen atoms in a range of coordination environments in polyoxometalates is nearly constant,[6] slightly exceeding the classical value of two.

In this paper, we extend the utility of the Mayer bond order to cover interactions between fragments and between groups of symmetry-equivalent fragments. The analytical method presented is applicable to any single-determinant MO model but is most immediately related to the approach used by the widely used Amsterdam density functional (ADF) code.[10] After presenting these extensions of the Mayer bond order, their usefulness in the computational analysis of bonding in some simple organometallic sandwich complexes is examined.

Analytical approach: Although atomic and diatomic quantities prove very useful in conveying chemically transparent notions from the results of high-level calculations, much of chemistry is best understood in terms of building blocks other than the atom. Molecules can often be usefully imagined as being built from fragments, such as ligands and metals, functional groups and hydrocarbon backbones, and donor and acceptor groups. The work of Hoffmann,[2] Albright, Burdett and Whangbo,[3] amongst many others, has shown just how powerful this approach is and how it can be used to relate the chemistry of apparently disparate parts of the periodic table. Scheme 1 shows some examples of typical

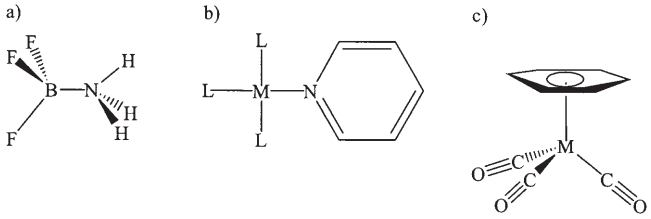

Scheme 1. Typical Lewis acid–base adducts.

interactions, which are better considered as between fragments rather than atoms. Scheme 1a shows a typical Lewis acid–base adduct. As suggested by this description of the molecule, it is perhaps most natural to imagine the bonding between the orbitals of the pyramidal BF_3 and the NH_3 fragments, rather than between the orbitals of the B and N atoms. Scheme 1b shows a typical metal–ligand interaction. Again, it seems more appropriate to consider the bonding between a ML_3 unit and a pyridine ligand rather than that between a metal and a nitrogen atom. Indeed, the influence of ligand-field treatments of bonding, such as the angular overlap model[11] (AOM) and cellular ligand-field[12] (CLF) model, is such that the interaction is measured by the σ and π-donor or π-acceptor character of the ligand, rather than of the donor atom. Scheme 1a shows a typical organometallic complex. It is perfectly possible to calculate the bond order between the metal and the individual ring carbon atoms and to construct localized M–C orbitals. It is more appropriate, however, to describe the bonding in terms of an interaction between an arene ring and a $M(CO)_3$ fragment. In this way, the delocalized π-orbitals of the ring interact with the suitably orientated frontier orbitals of the pyrami-

dal $M(CO)_3$ unit. The bonding is then considered as ring-to-metal σ and π donation with metal-to-ring δ backdonation utilizing appropriate occupied and empty frontier orbitals on the two fragments.

MOs, θ, are commonly constructed as linear combinations of atomic orbitals, γ, as shown in Equation (4), in which c_{iA} is the coefficient for the *i*th atomic orbital on atom A, and the first summation is over all atoms in the molecule.

$$\theta = \sum_{A}^{\text{molecule}} \sum_{i}^{\text{on A}} c_{iA}\gamma_{iA} \tag{4}$$

As noted above, it is often natural to group the atoms in a molecule into fragments. It is similarly possible to partition the basis set of atomic orbitals into those belonging to each fragment and calculate the optimum linear combinations, ϕ, for each fragment, as outlined in Equation (5), in which the first summation is restricted to the atoms chosen to belong to the fragment.

$$\phi = \sum_{A}^{\text{on f}} \sum_{i}^{\text{on A}} c'_{iA}\gamma_{iA} \tag{5}$$

All of the fragments are taken to have the geometries that they adopt in the final molecules, as in Hoffmann's fragment and isolobal approaches,[2] so that these "fragment orbitals" (FOs) reflect the directional characteristics and energies of the orbitals used to form the molecule. The MOs can then be constructed as linear combinations of the fragment orbitals, Equation (6), in which c''_{if} are the coefficients for the *i*th FO on fragment f.

$$\theta = \sum_{f}^{\text{molecule}} \sum_{i}^{\text{on f}} c''_{if}\phi_{if} \tag{6}$$

The bond order between the fragments [Eq. (7)] can be defined analogous to Equation (1) on the basis of fragment orbitals.

$$\beta_{f_1f_2}(\text{FO}) = \sum_{i}^{\text{on f}_1} \sum_{j}^{\text{on f}_2} (\mathbf{PS})_{ij}(\mathbf{PS})_{ji} \tag{7}$$

The **PS** matrix is constructed on this basis. The total bonding power of a fragment can similarly be defined through its covalency, the sum of its bond orders and its total valency.

The MOs in the fragment-orbital basis are related to those in the atomic-orbital basis by a unitary transformation, Equation (8), in which **C** and **C**′′ represent the matrix of orbital coefficients in the atomic orbital and fragment orbital bases respectively and **U** is determined by the choice of fragments.

$$C'' = \mathbf{UC} \tag{8}$$

The **PS** matrix in the fragment orbital basis is then related to that in the atomic orbital (AO) basis by a similar transformation [Eq. (9)].

$$\mathbf{PS}^{\text{FO}} = \mathbf{U}(\mathbf{PS})^{\text{AO}}\bar{\mathbf{U}} \tag{9}$$

As, by definition, an atom cannot belong to more than one fragment, the bond order between two fragments is therefore equal to the sum of the diatomic bond orders between the atoms constituting each fragment.

As well as reflecting the number of shared electron pairs between fragments, the bond order can be used to assess which of the fragment orbitals, occupied and empty, are important in the bonding between the fragments. The bond order given in Equation (7) is a sum of the contributions from each combination of the orbitals on the two fragments. The largest terms in the summation can thus be used to identify the key frontier orbitals involved in the interaction. Although such information is available by visualizing or studying the MOs given by Equation (6), the bond order includes contributions from all the occupied levels and so is much simpler to routinely use, especially for large systems. It also gives a quantitative measure of the key orbital interactions. A typical use of the fragment bond order would be the calculation of the σ and π contributions to the Cr–CO bond order in any molecule containing a Cr–CO bond. The relative importance of the CO 1σ, 2σ and 3σ orbitals to the σ bonding and of the CO 1π and 2π orbitals to the π bonding can be assessed.

As for the diatomic bond order, the bond order between fragments can be expressed, in many systems, as a sum over symmetry species Γ [Eq. (10)].

$$\beta_{f_1f_2}(\text{FO}) = \sum_{\Gamma} \beta^{\Gamma}_{f_1f_2}(\text{FO}) \tag{10}$$

Decomposition allows the calculation of the separate σ and π contributions. The summation does not apply when a pair of orbitals on two fragments occurs in more than one symmetry species. This can occur where fragments are equivalent by symmetry. For example, fragmenting C_6H_6 into six CH units does not allow the a_{2u} and e_{1g} π bond orders to be calculated, as the same fragment orbitals are involved in both symmetry species. However, the in-plane "σ" and out-of-plane "π" bond orders can be established by lowering the symmetry to C_s to remove the equivalence of the CH groups.

For molecules involving groups of symmetry-equivalent fragments, symmetry-adapted linear combinations of the fragment orbitals, or "symmetrized fragment orbitals", ψ, (SFOs) can be constructed by using Equation (11), in which c'''_{if} are the symmetry determined coefficients for the *i*th FO on fragment f and the summation is over all symmetry-equivalent fragments.

$$\psi = \sum_{i}^{\text{on f}} c'''_{if}\phi^{\text{FO}}_{if} \tag{11}$$

The MOs can then be calculated as combinations of the SFOs on different groups. The bond order between the group g_1 and g_2 can be defined analogously to that given in Equations (1) and (7) on the basis of SFOs [Eq. (12)], in which the **PS** matrix is constructed in this basis.

$$\beta_{g_1 g_2}(\mathrm{SFO}) = \sum_{i}^{\text{on } g_1} \sum_{j}^{\text{on } g_2} (\mathbf{PS})_{ij}(\mathbf{PS})_{ji} \qquad (12)$$

The fragments can, of course, simply be atoms. On this basis, the bond orders are naturally decomposed into the contributions from different symmetries. The bond order on this basis relates naturally to symmetry-based views of bonding. A typical use of the SFO bond order would be the calculation of the a_{1g}, t_{1u}, e_g and t_{2g} contributions to the Cr–$(CO)_6$ bond order in octahedral $Cr(CO)_6$.

Computational Methods

All density functional (DF) calculations reported in this work were performed with the ADF 2000.02 program[13] using a triple-ζ Slater-type orbital (STO)[14] framework incorporating frozen cores (ADF TZP C.1s, Mg.1s, Ca.2p, Sr.3d, Ba.4d, Fe.2p, Cr.2p, Mn.2p, Co.2p, Ni.2p, Ce.5p, Th.5d, Mo.4p, W.4f, B.1s, N.1s) and the zeroth-order regular approximation (ZORA) relativistic correction.[15] The Vosko, Wilk and Nusair (VWN)[16] local density approximation (LDA)[17] and the BP86 density functional, which utilizes the exchange correction proposed by Becke[18] and the correlation term put forward by Perdew,[19] were used in all DF calculations. The bond order and valency indexes were obtained according to the definitions proposed by Mayer[7] and by Evarestov and Veryazov,[9] respectively by using the MAYER program,[20] which was written and specifically extended by the authors to facilitate calculation of the Mayer bond order between molecular fragments from the ADF output. All charges given were calculated by using Mulliken's definition.

In this paper, the bonding in a number of archetypal organometallic compounds is re-examined by using this approach. The symmetrical sandwich complexes $[M(\eta^5\text{-}C_5H_5)_2]$(M=Mg, Ca, Sr, Ba, Fe) and $[Cr(\eta^6\text{-}C_6H_6)_2]$ and the unsymmetrical sandwich complexes $[M(\eta^5\text{-}C_5H_5)(\eta^x\text{-}C_xH_x)]$ (M=Cr; x=7, M=Mn; $x=6$, M=Co; $x=4$, M=Ni; $x=3$) have been studied using this approach. Whilst the bonding in this set is fairly well understood, these molecules are of sufficiently broad interest and complexity to allow the present approach to be illustrated using a variety of chemically intuitive fragments.

To calculate bond orders between fragments, such as between the metal and the polyene rings or the $M(CO)_x$ and the polyene ring, the FOs for each of the user-defined fragments are first calculated (generating ADF TAPE21 files). The MOs of the complete molecule are then obtained using the FO basis set. The bond orders are obtained directly and rapidly from the ADF output file using the MAYER program.[20]

Further insight into the bonding can be afforded if the molecular bonding or atomization energy (E_B) is decomposed as, in Equation (13), in which E_O, E_P and E_E represent orbital mixing, Pauli repulsion and electrostatic interaction terms, respectively.

$$E_B = E_O + E_P + E_E \qquad (13)$$

Descriptions of the physical significance of these properties have been given by Landrum, Goldberg and Hoffmann[21] and Baerends and coworkers.[15,22] Both E_O and E_P arise from orbital-interaction effects with the former stabilizing and the latter destabilizing. E_O represents the effect of charge transfer, orbital mixing and polarization when filled and empty atomic orbitals overlap. This term can be decomposed as a sum over symmetry species Γ [Eq. (14)]

$$E_O = \sum_{\Gamma} E_0^{\Gamma} \qquad (14)$$

The E_P component is obtained by the requirement of antisymmetry and can be considered as the effect of the interaction between filled orbitals. The resulting destabilization, labelled as Pauli exchange or overlap repulsion, has been described as a measure of steric interaction. The E_E contribution arises from the Coulombic interaction between the atoms, before any orbital relaxation occurs. It is dominated by nucleus–electron attractions.

The molecular-bonding energy can also be related to the change in energy when fragments, other than atoms, are brought together [Eq. (15)]

$$\Delta E_B = \Delta E_O + \Delta E_P + \Delta E_E \qquad (15)$$

The terms now represent the changes in orbital interaction, Pauli and electrostatic energies. We have previously studied the correlation between the bond order and valency indices and the orbital-interaction energy in polyoxometalates.[5,6] In this paper, this work is extended to compare the fragment bond orders with the fragment orbital-interaction energies.

Results and Discussion

$[M(\eta^5\text{-}C_5H_5)_2]$ (M=Mg, Ca, Sr, Ba and Fe): The preparation of ferrocene in the early 1950s initiated an explosion of interest in organometallic chemistry and its symmetrical shape with parallel rings still has the power to astonish. Isostructural $[M(\eta^5\text{-}C_5H_5)_2]$ molecules and derivatives are known for many transition metals and main-group metals. In this section, the bonding in ferrocene itself and the bis(η^5-cyclopentadienyl) complexes of the heavier alkaline earths are examined by using the fragment bond-order and bond-decomposition approaches.

Geometrical parameters for the optimized structures and a comparison with known experimental data are listed in Table S1 in the Supporting Information. Optimised structures for the alkaline-earth systems are in excellent agreement with those recently reported by Rayón and Frenking[23] using the same combination of the BP86 density functional and triple-ζ STO framework. We previously reported[24] calculations on these systems which indicate a tendency for the rings to bend away from being parallel for the heavier alkaline earths. The present calculations do not support this finding, which appears to be due to the higher quality of the basis sets used in the present work. The effects of bending are discussed in more detail below.

Figure 1a shows a qualitative molecular-orbital diagram for ferrocene. The diagram follows the approach common to many textbooks and undergraduate courses in building the MOs by first taking in-phase and out-of-phase combinations of the C_5H_5 π orbitals to produce the gerade and ungerade symmetry-adapted linear combinations (SALCs) of the $(\eta^5\text{-}C_5H_5)_2^{2-}$ fragment. These SALCs are then combined with the matching orbitals on the metal, commonly taken to be an Fe^{2+} ion. The occupied a_{1g} and a_{2u} orbitals of the $(\eta^5\text{-}C_5H_5)_2^{2-}$ fragment can be considered to "σ donate" into the metal a_{1g} (4s and $3d_{z^2}$) and a_{2u} ($4p_z$) orbitals. Similarly, the e_{1g} and e_{1u} orbitals of the organic fragment can be consid-

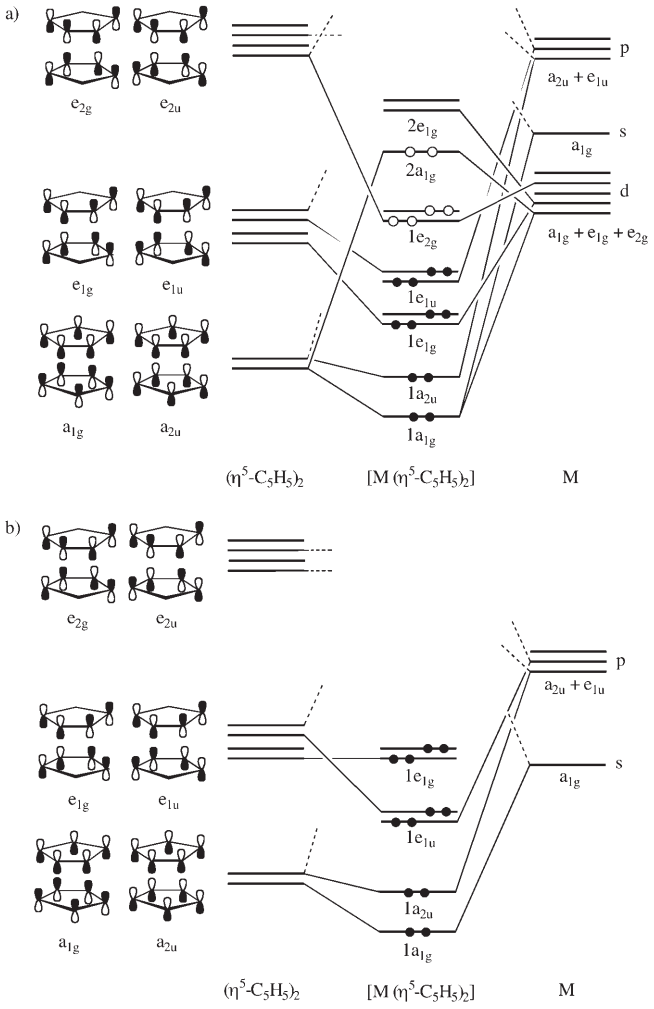

Figure 1. Qualitative MO scheme for $[M(\eta^5\text{-}C_5H_5)_2]$ sandwich complexes, in which a) M is a transition metal and b) M is a main-group metal.

ered to "π donate" into the metal $3d_{xz,yz}$ and $4p_{x,y}$ orbitals respectively. Finally, the metal $d_{x^2-y^2,xy}$ orbitals can be considered to "δ backdonate" into the vacant e_{2g} orbitals on the rings. Table 1 lists the bond orders and orbital interaction energies between the Fe and $(\eta^5\text{-}C_5H_5)_2$ fragments, decomposed into the σ, π and δ components. Note that as the bond orders are calculated from the final density matrix they are not dependent on the charges or spins that a chemist's intuition might arbitrarily place on the fragments. The orbital-interaction energies are highly dependent on the choice of fragment charges and, in principle, spins.

The charge on Fe in the complex is very low (ca. 0.02), indicating that the interaction is essentially covalent in nature. The total bond order between Fe and the $(\eta^5\text{-}C_5H_5)_2$ fragments is 4.9, indicating covalence and valence of about 2.5 for each ring or 0.5 for each C atom. This is achieved through contributions of 1.0, 2.8 and 1.2 from σ, π and δ interactions, respectively. This decomposition is consistent with the contributions to the bond energy and also suggest that the π and δ interactions dominate.

The σ bonding is made from contributions of 0.4 and 0.6 from the a_{1g} and a_{2u} orbitals, respectively. The a_{1g} contribution arises from three main orbital interactions. The Fe $3d_{z^2}$ orbital weakly interacts with a ring σ* orbital involving a combination of H 1s orbitals, shown in Figure 2a, giving a bond order of 0.1. The Fe 4s orbital interacts with the ring π orbital shown in Figure 1a, in an antibonding manner, and with the ring C–H bonding orbital shown in Figure 2b, giving contributions of 0.5 and −0.3, respectively. The bond-order analysis also shows a small, stabilizing hybridization between the Fe $3d_{z^2}$ and 4s orbitals. The a_{2u} bonding arises through interaction of the Fe $4p_z$ with a ring σ orbital, shown in Figure 2c, and with the ring π orbital, shown in Figure 1a, leading to contributions of 0.2 and 0.3, respectively. The small role of the Fe $3d_{z^2}$ orbital has been recognized.[3] The analysis, however, also reveals the role of the ring σ orbitals in an analytically straightforward way.

The π bonding is made from contributions of 2.0 and 0.8 from the e_{1g} and e_{1u} orbitals, respectively. Both of these arise in turn from the interactions shown in Figure 1a between the Fe valence orbitals and the ring π orbitals of appropriate symmetry. A δ bonding of 1.2 similarly arises from the interaction, shown in Figure 1a, between the Fe $3d_\delta$ orbitals and the matching ring π functions. The e_{1g} bond order suggests that this π contribution to the bonding is significant. Consistent with this, the orbital-interaction energy for this term is also large and appears to dominate the bond energy. The importance of π donation from the ligands into empty metal d orbitals is also indicated by the results obtained for the other transition-metal sandwich complexes discussed below.

The bonding in ferrocene, revealed by the fragment bond-order analysis, is thus consistent with the familiar MO diagram for the π and δ bonding, but is slightly more complicated for the σ interactions, in which the ring σ functions also contribute. The bond-order and bond-energy analyses indicate that π and δ bonding and hence the metal 3d ring π orbital interaction dominate.

Table 1. Fragment bond orders (β), orbital interaction energies (ΔE_O) and metal charges (q_M) for $[M(\eta^5\text{-}C_5H_5)_2]$ (M = Mg, Ca, Sr, Ba and Fe) for the $(\eta^5\text{-}C_5H_5)_2$ and M fragments.

		σ		π		δ	total	q_M
		a_{1g}	a_{2u}	e_{1g}	e_{1u}	e_{2g}		
$[Mg(\eta^5\text{-}C_5H_5)_2]$	β_{AB} (FO)	0.60	0.46	0.57	0.92	0.07	2.62	0.49
	ΔE_O	−163	−110	−197	−246	−52	−815	
$[Ca(\eta^5\text{-}C_5H_5)_2]$	β_{AB} (FO)	0.10	0.08	0.31	0.36	0.00	0.85	1.57
	ΔE_O	−91	−54	−270	−124	−40	−614	
$[Sr(\eta^5\text{-}C_5H_5)_2]$	β_{AB} (FO)	0.036	0.07	0	0.28	0	0.38	1.80
	ΔE_O	−67	−43	−108	−98	−29	−373	
$[Ba(\eta^5\text{-}C_5H_5)_2]$	β_{AB} (FO)	−0.02	−0.01	0	0.12	0	0.09	1.93
	ΔE_O	−52	−32	−98	−75	−24	−306	
$[Fe(\eta^5\text{-}C_5H_5)_2]$	β_{AB} (FO)	0.43	0.57	2.00	0.77	1.15	4.91	0.03
	ΔE_O	−203	−118	−1556	−258	−208	−2413	

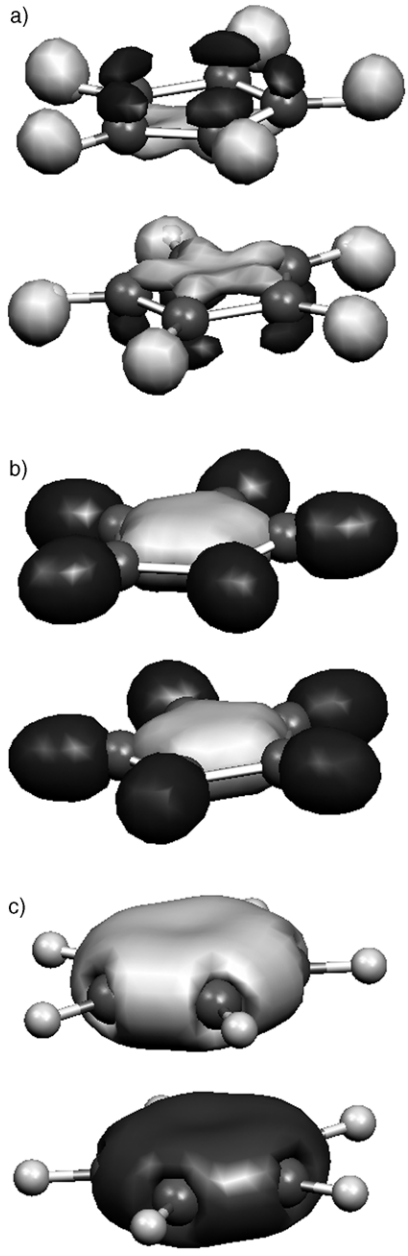

Figure 2. a) C–H σ^*, b) C–H σ and c) C 2s dominated σ ligand-group orbitals for the $(\eta^5\text{-}C_5H_5)_2$ fragment.

Figure 1b shows a qualitative MO diagram for a D_{5d} [M-$(\eta^5\text{-}C_5H_5)_2$] complex in which the metal has only s and p orbitals in its valence shell, constructed in a similar way to that used for Figure 1a, in which the metal also uses d orbitals. Without d orbitals on the metal, the δ interaction is lost. This diagram might be expected to be relevant for [Mg-$(\eta^5\text{-}C_5H_5)_2$] as the contribution from the Mg orbitals might be expected to be minimal. The remaining alkaline-earth metals are placed immediately before the transition-metal block in the periodic table, so they might be expected to have important contributions from metal d orbitals.[26] Table 1 lists the contributions to the bond order and orbital interaction energies for the [M($\eta^5\text{-}C_5H_5)_2$] (M = Mg, Ca, Sr, Ba) complexes.

The metal charges indicate that ionicity is important in all the complexes and that this increase as Group 2 is descended, with [Ba($\eta^5\text{-}C_5H_5)_2$] being essentially $Ba^{2+}[(\eta^5\text{-}C_5H_5)_2]^{2-}$ The bond orders and orbital interaction energies are also consistent with this observation, being significantly smaller than for ferrocene and decreasing rapidly down the group.

For [Mg($\eta^5\text{-}C_5H_5)_2$], the covalence of the ring is 2.6. The σ bonding represents a slightly higher proportion of the total interaction than in ferrocene. The orbital interaction energies are consistent with this observation. The a_{1g} interaction is dominated by an overlap between the Mg 3s and the appropriate ring π orbital, shown in Figure 1b. The a_{2u} interaction is similarly dominated by an interaction between the Mg $3p_z$ orbitals and the appropriate ring π orbital, shown in Figure 1b. The interaction between Mg $3p_z$ and a ring σ orbital, similar to that shown in Figure 2c, contributes about a quarter of the overall bond order. The π bonding contains contributions from both the e_{1g} and e_{1u} representations. The contribution from the former is somewhat surprising as it arises from interactions between the Mg $3d_\pi$ orbitals and ring σ and π orbitals. The orbital interaction energies also indicate a significant contribution from this source. The largest contribution to the bonding arises from the e_{1u} interaction between the Mg $3p_\pi$ orbitals and the matching ring π orbitals, shown in Figure 1b.

In the remaining alkaline-earth complexes, there is a considerable decrease in the σ bonding. In [Ca($\eta^5\text{-}C_5H_5)_2$], π bonding arises through both its $3d_\pi$ and $4p_\pi$ orbitals overlapping with the matching ring π orbitals, whilst only the p_π orbitals appear to be important in the Sr and Ba complexes. In a previous publication,[26] we reported that the d_π orbitals are important in causing the bent geometry of the heavier alkaline earth metallocenes. Whilst the present work also suggests that the d_π–ring π orbital interaction increases on bending, the small role of these orbitals and the large ionicity predicted by the larger basis set used in the present work presumably critically reduces this role, so that geometry with parallel rings is predicted.

We have previously commented on the reproducibility of the oxygen total valence in a variety of sites and coordination numbers in polyoxometalates.[6] The valency of the carbon atoms in the metallocenes discussed in this section is also consistent, this is, about four, despite the variations in the ionicity of the complexes. The total valence of the η^5-C_5H_5 ligand, however, decreases from approximately 2.5 in [Fe($\eta^5\text{-}C_5H_5)_2$] to 0.1 in [Ba($\eta^5\text{-}C_5H_5)_2$]. This variation underlines the flexibility in the bonding of the cyclopentadienyl ligand. The synergistic nature of the metal–ring interaction means that increases in the π and δ interactions have a direct effect on the C=C bonding, with the C–C bond order decreasing from 1.4 in $(\eta^5\text{-}C_5H_5)_2$Ba to 1.1 in $(\eta^5\text{-}C_5H_5)_2$Fe, so that the carbon valence is maintained.

[Cr(η^6-$C_6H_6)_2$Cr]: [Cr($\eta^6\text{-}C_6H_6)_2$] is the benzene ring analogue of ferrocene and Figure 3 shows a qualitative MO dia-

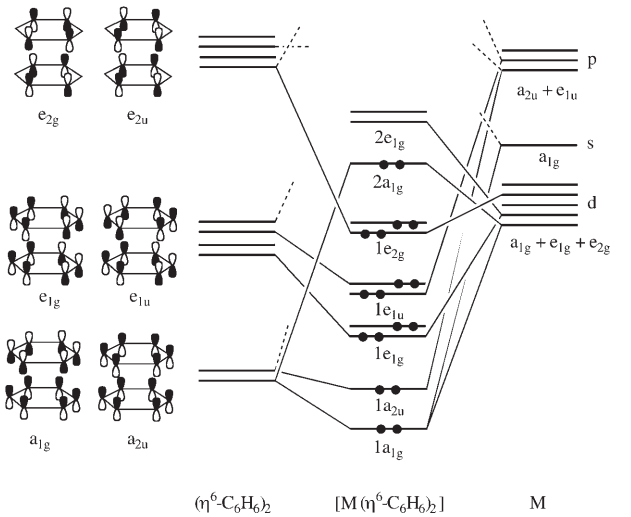

Figure 3. Qualitative MO scheme for a $[M(\eta^5\text{-}C_6H_6)_2]$ sandwich complex of a transition metal.

gram for this complex, showing the isolobal nature of the bonding in these molecules. Geometrical parameters for the optimized structure and a comparison with known experimental data are listed in Table S1 in the Supporting Information. The MO diagram follows the approach used above for bis(cyclopentadienyl) complexes and in common with many textbooks and undergraduate courses of building the MOs by first taking in-phase and out-of-phase combinations of the C_6H_6 π orbitals to produce the gerade and ungerade symmetry-adapted linear combinations (SALCs) of the (η^6-C_6H_6) fragment. These SALCs are then combined with the matching orbitals on the metal, commonly taken to be a neutral Cr atom.

The occupied a_{1g} and a_{2u} orbitals of the ligand fragment can be considered to "σ donate" into the metal a_{1g} (4s and $3d_{z^2}$) and a_{2u} ($4p_z$) orbitals. Similarly, the e_{1g} and e_{1u} orbitals of the organic fragment can be considered to "π donate" into the metal, $3d_{xz,yz}$ and $4p_{x,y}$ orbitals, respectively. Finally, the metal $d_{x^2-y^2,xy}$ orbitals can be considered to "δ backdonate" into the vacant e_{2g} orbitals on the rings. Table 2 lists

Table 2. Fragment bond orders (β) and metal charges (q_M) for $[Cr(\eta^6\text{-}C_6H_6)_2]$ for the $(\eta^x\text{-}C_xH_x)_2$ and M fragments.

	σ		π		δ	total	q_M
	a_{1g}	a_{2u}	e_{1g}	e_{1u}	e_{2g}		
$[Cr(\eta^6\text{-}C_6H_6)_2]$	0.42	0.47	1.80	0.79	1.98	5.26	−0.06

the bond orders and orbital interaction energies between the metal and the ligands, decomposed into σ, π and δ components. The charge on Cr in the complex is very low (ca. −0.06), indicating that the interaction is, like ferrocene, essentially covalent in nature. The total bond order between Cr and the $(\eta^6\text{-}C_6H_6)_2$ fragments is 5.3, indicating a covalence and valence of about 2.7 for each ring or 0.4 for each C atom. This is achieved through contributions of 0.9, 2.4 and 2.0 from σ, π and δ interactions, respectively, suggesting slightly weaker π but stronger δ interactions than in ferrocene, 1.0, 2.8 and 1.2 from σ, π and δ interactions, respectively. This decomposition is consistent with the contributions to the bond energy, which also suggest that π and δ interactions dominate.

The σ bonding is made from contributions of 0.4 and 0.6 from the a_{1g} and a_{2u} orbitals, respectively. The a_{1g} interaction is dominated by a bond with order 0.2 between the Cr $3d_{z^2}$ orbital and the C–H σ* orbital, analogous to that shown in Figure 2a for ferrocene, a bond with order 0.3 between Cr 4s and the ring π orbital shown in Figure 3 and an antibond with order −0.2 between the Cr 4s and a ring σ orbital, analogous to that shown in Figure 2b for ferrocene. The interaction between the Cr $3d_{z^2}$ orbital and the ring π orbital contributes only about 0.01 of a bond. The a_{2u} interaction is dominated by similar contributions from the Cr $4p_z$ orbital overlapping with a ring σ orbital, analogous to that shown in Figure 2c for ferrocene, and the ring π orbital shown in Figure 3.

The π bonding is made from contributions of 1.8 and 0.8 from the e_{1g} and e_{1u} orbitals, respectively. The e_{1g} interaction is dominated by a Cr $3d_\pi$ ring π orbital overlap. Significant contributions to the e_{1u} bonding arise from the Cr $4p_\pi$ orbitals overlapping with the ring π orbitals and the ring C–H σ* function, which have bond orders of 0.6 and 0.2, respectively. The δ bonding is dominated by the interaction between the metal $3d_\delta$ orbital and the matching ring π function, as shown in Figure 3.

The bonding in chromocene revealed by the fragment bond-order analysis is again consistent with the familiar MO diagram for π and δ bonding, but is slightly more complicated for the σ interactions, in which the ring σ functions are again shown to contribute. As in ferrocene, the π and δ interactions dominate.

$[Cr(\eta^5\text{-}C_5H_5)(\eta^7\text{-}C_7H_7)]$, $[Mn(\eta^5\text{-}C_5H_5)(\eta^6\text{-}C_6H_6)]$, $[Fe(\eta^5\text{-}C_5H_5)(\eta^5\text{-}C_5H_5)]$ and $[Co(\eta^5\text{-}C_5H_5)(\eta^4\text{-}C_4H_4)]$ and $[Ni(\eta^5\text{-}C_5H_5)(\eta^3\text{-}C_3H_3)]$: In the previous sections, the utility of the fragment bond-order approach for analyzing the bonding in high-symmetry sandwich complexes was outlined. In this section, the use of the approach will be demonstrated for systems in which low symmetry masks the relatively simple underlying orbital structures. Together with ferrocene, the mixed sandwich complexes $[M(\eta^5\text{-}C_5H_5)(\eta^x\text{-}C_xH_x)]$ (M = Cr; $x = 7$, M = Mn; $x = 6$, M = Co; $x = 4$, M = Ni; $x = 3$) form a convenient set of isoelectronic molecules that fit this description. These mixed sandwich complexes can have, at most, C_s symmetry, but, as revealed by the isolobal and orbital interaction approaches,[2,3] have MOs that are closely related to those in the high-symmetry ferrocene complex. Following this work, it is most convenient to consider the bonding in terms of the interaction of the $[M(\eta^5\text{-}C_5H_5)]$ fragment with the orbitals of the second ring. Table S2 in the Supporting Information lists the optimized M–C bond lengths and

Table 3 lists the calculated fragment bond orders for these molecules.

Table 3. Fragment bond orders (β) and metal charges (q_M) between [M(η^5-C_5H_5)] and C_xH_x rings (M = Cr; x = 7, M = Mn; x = 6, M = Co; x = 4, M = Ni; x = 3) fragments.

	σ	π	δ	total	q_M
[Cr(η^5-C_5H_5)(η^7-C_7H_7)]	0.5	0.9	1.9	3.3	−0.003
[Mn(η^5-C_5H_5)(η^6-C_6H_6)]	0.5	1.0	1.4	3.3	0.003
[Fe(η^5-C_5H_5)(η^5-C_5H_5)]	0.6	1.4	0.6	2.6	0.03
[Co(η^5-C_5H_5)(η^4-C_4H_4)]	0.5	1.8	0.1	2.4	0.11
[Ni(η^5-C_5H_5)(η^3-C_3H_3)]	0.4	1.6	0	2.0	0.22

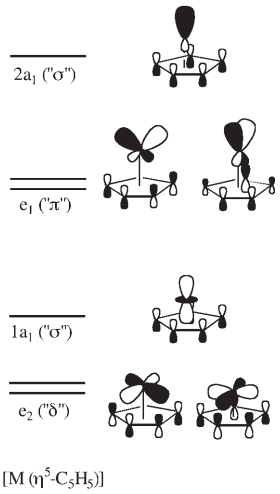

Figure 4. Frontier orbitals for a [M(η^5-C_5H_5)] fragment.

Figure 4 shows the frontier orbitals of the C_{5v} [M(η^5-C_5H_5)] fragment. The valence orbitals are $e_2+1a_1+e_1+2a_1$, with the e_2+1a_1 levels filled for a d^6 metal ion. The e_2 levels are δ bonding between the metal and C_5H_5 ring and also present a δ orientation to the second ring. The $1a_1$ orbital is primarily metal $3d_{z^2}$ in character and has the possibility of forming a σ interaction with the second ring. The e_1 orbitals are π bonding between metal and C_5H_5 but, because of d–p hybridization on the metal are shaped to form a strong π interaction with a ring placed above the fragment. Similarly, because of s–p hybridization, the $2a_1$ orbital is fashioned to σ interact with the second ring.

Figure 5 shows the familiar π orbitals of the C_xH_x rings with x = 3–7. Each is labelled with the pseudosymmetry of a linear ligator. Thus, C_3H_3 presents orbitals of σ and π symmetry to the [M(η^5-C_5H_5)] fragment. C_4H_4 and C_5H_5 additionally offer a single and pair of δ orbitals, respectively. Likewise, C_6H_6 and C_7H_7 have a single and a pair of φ orbitals, respectively, which are unable to interact with the fragment. There is a good match between the orbitals on the second ring and the valence orbitals of the [M(η^5-C_5H_5)] fragment. The relative importance of the interactions between these frontier orbitals can be gauged using the fragment bond-order approach.

The C_s symmetry of the mixed-sandwich complexes means that other orbital interactions are possible. In the complex, the σ-type orbitals of (η^5-C_5H_5)M have a′ symmetry, whilst the π and δ-type orbitals split into a′ + a″. Similarly, the σ-type orbitals of the second ring have a′ symmetry, and the π and δ orbitals split into a′ + a″. The importance (or not) of the interactions between all a′ orbitals and between all a″ orbitals is revealed by the fragment bond-order analysis. Additionally, the role played by the remaining orbitals of each fragment is also evident from the analysis, as discussed above for the symmetrical-sandwich complexes.

For [Cr(η^5-C_5H_5)(η^7-C_7H_7)], the Cr–C bond orders are 0.39 and 0.49 for the five and seven-membered rings, respectively. As might be expected, the bonding between [Cr(η^5-C_5H_5)] and C_7H_7 is dominated by the interactions between the frontier orbitals shown in Figure 4 and Figure 5, for the π and δ-type interactions but not for the σ-type interactions.

The σ-type interaction is represented entirely within the a′ orbitals of the complex. There is a bond order of 0.16 between the $1a_1$ d_{z^2}-dominated function of the [Cr(η^5-C_5H_5)] unit and two empty orbitals of the C_7H_7 ring, which are dominated by the hydrogen s orbitals analogous to that shown in Figure 2a for a five-membered ring. These interactions are presumably a primary cause of the pronounced distortion of the seven-membered ring to allow closer Cr–H interaction. Only very small bond orders arise from interaction of the [Cr(η^5-C_5H_5)] $1a_1$ fragment orbital with the π functions of C_7H_7, as the latter are located around the nodal cone of the chromium d_{z^2} orbital. The empty $2a_1$ orbital of the [Cr(η^5-C_5H_5)] fragment, which is essentially an chromium-based sp hybrid directed towards the seven-membered ring, forms a bonding interaction with the a_2'' π orbital of the latter, giving rise to a bond order of 0.19. The same orbital also interacts with a low-lying combination of the carbon 2s orbitals of the C_7H_7 ring, leading to a bond order of 0.09. The σ-type interactions between the two fragments thus arise from [Cr(η^5-C_5H_5)] donation to C_7H_7 hydrogen-based acceptor functions and from π and σ-bonding electron density on C_7H_7 being donated to [Cr(η^5-C_5H_5)]. Thus,

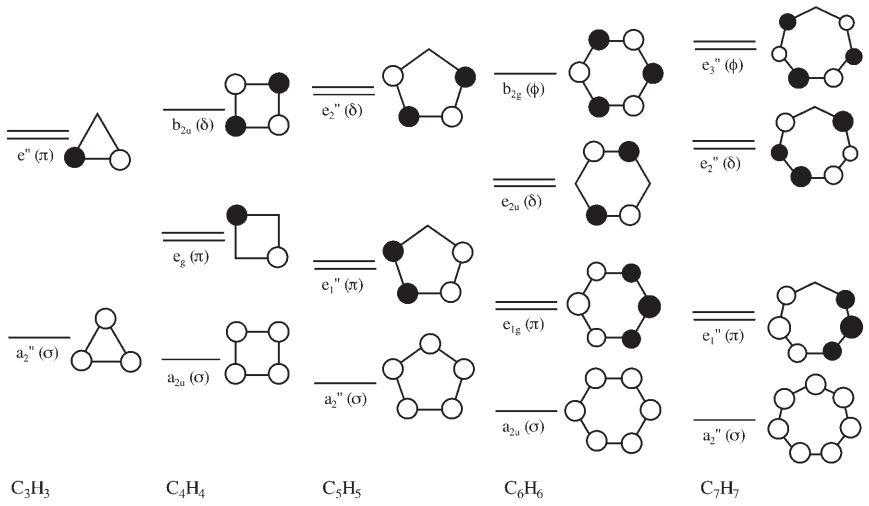

Figure 5. π orbitals for organic ring systems (shown from above).

σ-type bonding is drawn from both σ and π orbitals of the C_7H_7 ring with similar levels of importance. Despite the low symmetry of the overall complex, the σ-type functions of the $[Cr(\eta^5\text{-}C_5H_5)]$ fragment do not interact significantly with the π, δ and ϕ functions of the C_7H_7 ring.

The π-type interaction between the two fragments is drawn from both a′ and a″ orbitals of the complex. It is dominated by the overlap of the d_{xz} and d_{yz}-like e_1 acceptor functions of the $[Cr(\eta^5\text{-}C_5H_5)]$ fragment with the e_1'' π orbitals of the C_7H_7 ring giving rise to bond orders of 0.37 for both the a′ and a″ overlaps. Essentially equal contributions from the formally a′ and a″ orbitals of the complex fully justify the description of the interaction as π-like. There are also small contributions, with bond orders of 0.1 from these same acceptor functions interacting with low-lying combinations of the carbon 2s orbitals on the C_7H_7 fragment.

The δ-type interaction is completely dominated by the interaction between the d_{xy} and $d_{x^2\text{-}y^2}$-like e_2 donor functions of the $[Cr(\eta^5\text{-}C_5H_5)]$ fragment with the e_2'' π orbitals of the C_7H_7 ring giving rise to bond orders of 0.95 for both the a′ and a″ orbitals of the complex. Again the similarity of these contributions fully justifies use of the δ pseudosymmetry label. Overall, the bond orders for the σ, π and δ-type interactions between the $[Cr(\eta^5\text{-}C_5H_5)]$ and C_7H_7 fragments are roughly of the order 0.5:0.9:1.9.

$[Mn(\eta^5\text{-}C_5H_5)(\eta^6\text{-}C_6H_6)]$ is isoelectronic to $[Cr(\eta^5\text{-}C_5H_5)(\eta^7\text{-}C_7H_7)]$. The frontier orbitals of $[Mn(\eta^5\text{-}C_5H_5)]$ are the same as for $[Mn(\eta^5\text{-}C_5H_5)]$, with the $1a_1$ level being the highest occupied orbital. The π orbitals of benzene are shown in Figure 5. C_6H_6 and C_7H_7 offer similar π functions to the metal fragment. Although C_7H_7 has an additional "ϕ-type" orbital to C_6H_6, there are, as noted above, no donor functions of appropriate symmetry and energy to interact so that this difference should not greatly affect the overall interaction. The Mn–C bond orders are 0.44 and 0.51 for the five- and six-membered rings, respectively. As described above for $[Cr(\eta^5\text{-}C_5H_5)(\eta^7\text{-}C_7H_7)]$, analysis reveals that π- and δ-type interactions are dominated by the interaction of the metal-based fragment orbitals with the π functions on the second ring, whereas other orbitals play a role in the σ-type interactions.

The σ-type interactions are again represented by the a′ orbitals of the complex. There is a bond order of 0.08 between the $1a_1$ d_{z^2}-dominated function of the $[Mn(\eta^5\text{-}C_5H_5)]$ unit and an empty orbital of the C_7H_7 ring, which is dominated by the hydrogen s orbitals analogous to that shown in Figure 2a for a five-membered ring. The analogous interaction is also present in $[Cr(\eta^5\text{-}C_5H_5)(\eta^7\text{-}C_7H_7)]$ and the large magnitude of the corresponding fragment bond order in the latter is reflected in a larger distortion of the seven-membered ring from planarity. Only very small bond orders arise from interaction of the $[Mn(\eta^5\text{-}C_5H_5)]$ $1a_1$ fragment orbital with π functions of the C_6H_6 ring, as again the latter are located around the nodal cone of the metal d_{z^2} orbital. The empty $2a_1$ metal sp-hybrid orbital of the $[Mn(\eta^5\text{-}C_5H_5)]$ fragment forms a bonding interaction with the a_{2u} π orbital of the benzene ring giving rise to a bond order of 0.19, almost the same as that found for the analogous interaction in $[Cr(\eta^5\text{-}C_5H_5)(\eta^7\text{-}C_7H_7)]$. The same metal-based fragment orbital also interacts with a low-lying combination of the carbon 2s orbitals of the C_6H_6 ring leading to a bond order of 0.17. The σ-type interactions between the two fragments thus arise from slightly weaker $[Mn(\eta^5\text{-}C_5H_5)]$ donation into C_6H_6 hydrogen-based acceptor functions; a similar degree of donation from C_6H_6 π-bonding electron density and somewhat great donation from C_6H_6 σ-bonding electron density into empty metal-based orbitals than in the chromium analogue. Again, the low symmetry of the overall complex does not lead to any significant mixing between the σ-type functions of the $[Mn(\eta^5\text{-}C_5H_5)]$ fragment with the π, δ and ϕ functions of the C_6H_6 ring.

The π-type interaction is dominated by overlap of the d_{xz} and d_{yz}-like e_1 acceptor functions of the $[Mn(\eta^5\text{-}C_5H_5)]$ fragment with the e_{1g} π orbitals of the C_6H_6 ring giving rise to bond orders of 0.50 for both the a′ and a″ overlaps. Again, essentially equal contributions from the formally a′ and a″ orbitals of the complex fully justifies the description of the interaction as π like. There are also small contributions, with bond orders of 0.06, from these same acceptor functions interacting with low-lying combinations of the carbon 2s orbitals on the benzene ring fragment.

The δ-type interaction is completely dominated by the interaction between the d_{xy}- and $d_{x}2_{-y}2$-like e_2 donor functions of the $[Mn(\eta^5\text{-}C_5H_5)]$ fragment with the e_{2u} π orbitals of the C_6H_6 ring giving rise to bond orders of 0.69 for both the a′ and a″ orbitals of the complex. Again the similarity of these contributions fully justifies use of the δ pseudosymmetry label.

Overall, the bond orders for the σ, π and δ-type interactions between $[Mn(\eta^5\text{-}C_5H_5)]$ and C_6H_6 fragments are roughly of the order 0.5:1.0:1.4, suggesting a strengthening of the π and a weakening of the δ-type interaction compared to the chromium system. The σ-type interaction is similar in the two systems although; as noted above, the C_6H_6 ring appears to be a slightly better donor and more reluctant acceptor of electron density into its σ and σ* orbitals, respectively, than the seven-membered ring.

The bonding in $[Fe(\eta^5\text{-}C_5H_5)_2]$ has been described above in terms of the interaction between the metal atom and the ligand-group orbitals of the rings. In this section, this description is augmented by examination of the interaction between the $[Fe(\eta^5\text{-}C_5H_5)]$ and C_5H_5 fragments. Unlike the other complexes in the isoelectronic systems described here, ferrocene has D_{5d} symmetry allowing full separation of the σ-, π- and δ-type interactions. As the two separate fragments each have C_{5v} symmetry, it is convenient to use this group in the description of the interaction between the fragments. The frontier orbitals of the $[Fe(\eta^5\text{-}C_5H_5)]$ and C_5H_5 fragments are shown in Figures 4 and 5. The Fe–C interatomic bond orders are 0.48.

The σ-type interactions occur in the a_1 orbitals of the complex. As in the other sandwich complexes, the doubly occupied metal d_{z^2}-dominated orbital $1a_1$ interacts with empty ring orbitals dominated by H 1s orbitals, rather than

ring π functions. The total bond order for this interaction of 0.05 is even smaller than that found for the manganese–benzene system, consistent with the only slight distortion of the C_5H_5 ring from planarity. The iron sp-hybrid function $2a_1$ interacts with a low-lying carbon 2s-dominated function to give a bond order of 0.17, essentially the same as noted above for the analogous interaction in the manganese system. The hybrid orbital also interacts with the a_2'' π function of the C_5H_5 ring leading to a bond order of 0.27, somewhat higher than that found in the manganese and chromium systems. The σ-type interactions between the two fragments thus arise from weaker $[Fe(\eta^5\text{-}C_5H_5)]$ donation into C_5H_5 hydrogen-based acceptor functions, a similar degree of donation from C_5H_5 σ-bonding electron density and a greater degree of C_5H_5 π-bonding electron density into empty metal-based orbitals than in the manganese analogue.

The π-type interaction occurs in the e_1 orbitals of the complex. As in the other sandwich complexes, it is dominated by the interaction between the e_1 frontier orbitals of the $[M(\eta^5\text{-}C_5H_5)]$ fragment and the corresponding π orbitals of the second ring. For ferrocene, the bond order between these doubly degenerate fragment orbitals is 1.42, suggesting an increase in the importance of π-type bonding along the series. The δ-type interaction occurs in the e_2 orbitals of the complex. It is dominated by the interaction between the e_2 frontier orbitals of the $[Fe(\eta^5\text{-}C_5H_5)]$ fragment with the empty e_2'' orbitals of the second C_5H_5 ring giving rise to an overall bond order of 0.58. It may be noted that the δ-type interaction is considerably smaller in $[Fe(\eta^5\text{-}C_5H_5)_2]$ than in $[Mn(\eta^5\text{-}C_5H_5)(\eta^6\text{-}C_6H_6)]$ despite the shorter Fe–C bond lengths in the former. This presumably reflects the lower energy of the relevant acceptor orbital on the C_6H_6 ligand than on the C_5H_5 ring. Overall, the bond orders for the σ, π and δ-type interactions between the $[Fe(\eta^5\text{-}C_5H_5)]$ and C_5H_5 fragments are roughly of the order 0.6:1.4:0.6, suggesting a further strengthening of the π-type interaction and weakening of the δ-type interaction compared to the manganese system.

$[Co(\eta^5\text{-}C_5H_5)(\eta^4\text{-}C_4H_4)]$ is the next isoelectronic complex in this series. The frontier orbitals of the $[Co(\eta^5\text{-}C_5H_5)]$ and C_4H_4 fragments are shown in Figures 4 and 5. The Co–C interatomic bond orders are 0.41 and 0.58 for the five- and four-membered rings, respectively.

The σ-type interactions occur in the a′ orbitals of the complex. Unlike the other sandwich complexes, the doubly occupied metal d_{z^2}-dominated orbital $1a_1$ does not interact significantly at all with empty orbitals of either σ* or π character and is essentially a non-bonding orbital. The cobalt sp-hybrid function $2a_1$ interacts with a low-lying carbon 2s-dominated function to give a bond order of 0.12, slightly smaller than for the other systems. The hybrid orbital interacts much more strongly with the a_{2u} π function of the C_4H_4 ring leading to a bond order of 0.34. Comparison with the analogous interaction in complexes of the lighter metals suggests that this interaction has increasing importance along the series. The σ-type interaction is thus dominated by donation from C_4H_4 π-bonding electron density into the empty metal-based $2a_1$.

The π-type interaction occurs in a′ and a″ orbitals of the complex. As in the other sandwich complexes, it is dominated by the interaction between the e_1 frontier orbitals of the $[M(\eta^5\text{-}C_5H_5)]$ fragment and the corresponding π orbitals of the second ring. The bond orders for the π-type interactions are 0.96 and 0.94 for a′ and a″ representations, respectively, indicating a further strengthening of the overall π-type interaction along the series. The δ-type interaction occurs only in the a′ orbitals of the complex as C_4H_4 has only one π orbital of the correct symmetry to interact in this fashion. The δ-type interaction is dominated by the interaction between one of the e_2 frontier orbitals of the $[Co(\eta^5\text{-}C_5H_5)]$ fragment with the empty b_{2u} orbital of the C_4H_4 ring giving rise to an overall bond order of only 0.13. Overall, the bond orders for the σ, π and δ-type interactions between the $[Co(\eta^5\text{-}C_5H_5)]$ and C_4H_4 fragments are roughly of the order 0.5:1.8:0.1, suggesting a further strengthening of the π-type interaction and weakening of the δ-type interaction compared to ferrocene.

The final molecule in this isoelectronic series is $[Ni(\eta^5\text{-}C_5H_5)(\eta^3\text{-}C_3H_3)]$. As shown in Figure 5, C_3H_3 only presents σ- and π-type orbitals to the metal fragment and these occur in the a′ and a′ + a″ orbitals of the complex, respectively. The Ni–C interatomic bond orders are calculated to be 0.33 and 0.63 for the five and three-membered rings, respectively.

The σ-type interactions are dominated by the interaction of the empty sp-hybrid type function on the nickel with donor functions on the C_3H_3 ring. Bond orders of 0.34 and 0.08 are calculated for the interaction of this function with the C_3H_3 a_2'' π orbital and a low-lying C 2s-dominated orbital, respectively. The former is very similar to that obtained for an analogous interaction in the cobalt system whilst the latter interaction appears to be reduced. The nickel d_{z^2}-dominated $1a_1$ function on the $[Ni(\eta^5\text{-}C_5H_5)]$ fragment is essentially non-bonding with very little interaction with empty H 1s orbital-dominated functions on the C_3H_3 ring. This interaction becomes consistently less important along the series.

The π interaction occurs between the e_1 functions on the $[Ni(\eta^5\text{-}C_5H_5)]$ fragment and the e″ orbitals on the C_3H_3 ring. The bond order is calculated to be 0.81 in both the a′ and a″ representations, suggesting a small decrease in this interaction compared to the cobalt complex.

With no ring functions of δ-type symmetry, the σ and π-type bond orders are roughly of the order 0.4:1.6.

Despite the low overall symmetry of these sandwich complexes, the fragment bond-order analysis allows an examination of the roles of σ-, π- and δ-type interactions and of the legitimacy of this description. The analysis also allows the suitability of the frontier orbital approach to be uncovered. Overall, the analysis suggests that the bonding in each complex is rather similar to that in the symmetrical-sandwich complexes ferrocene and chromocene described in earlier sections. The low symmetry of the present systems hides a relatively simple electronic structure, which is conveniently

analysed in terms of σ-, π- and δ-type interactions between the fragments. The σ-type interactions involve π, σ and σ* functions on the rings. For the complexes of the lighter metals, the interaction between the metal d_{z^2} orbital on the $[M(\eta^5\text{-}C_5H_5)]$ fragment and C-H σ* orbitals is important and contributes to bending of the hydrogen atoms on the second ring. Across the series, this metal orbital does not interact greatly with the ring π orbitals. A metal-based sp hydrid does interact with the π electrons on the second ring, but is also accepts electron density from σ orbitals on the second ring. The π- and δ-type interacts between the two fragments are dominated by the "classical" interaction between metal d functions and π orbitals on the second ring. Across the series, the π-type interaction appears to increase in importance, whereas the δ-type interaction decreases leading to an overall decrease in the interaction and a rise in the positive charge on the metal.

Conclusion

The fragment bond-order approach has been used to describe the bonding in a number of main-group and transition-metal sandwich complexes. By calculating the bond orders between molecular fragments rather than between atomic centres, this approach extends the utility of frontier-orbital and symmetry-theory techniques. For high-symmetry systems, the approach allows contribution from each irreducible representation to be analysed and thus provides a semiquantitative measure of the role of each bonding mode to the interfragment interactions. The validity of the frontier-orbital approach can also be gauged as the contributions from each fragment orbital interaction is included. This proves to be especially useful for low-symmetry complexes in which the symmetry of the fragment orbitals is formally lost. In the mixed-sandwich complexes studied, the approach shows that the electronic structure is very similar to that in the high-symmetry systems. Even in the low-symmetry systems, the roles of σ-, π- and δ-type interactions can be studied. The analysis also reveals the importance of σ and σ* orbitals on the rings and the role of the "classical" π functions.

Acknowledgements

The authors would like to thank EPSRC and the University of Hull for financial support.

[1] R. F. W. Bader, *Atoms in Molecules: a Quantum Theory*, Oxford University Press; Oxford, **1990**.
[2] R. Hoffmann, *Angew. Chem.* **1982**, *94*, 725; *Angew. Chem. Int. Ed. Engl.* **1982**, *21*, 711.
[3] T. A. Albright, J. K. Burdett, M.-H. Whangbo, *Orbital Interactions in Chemistry*, Wiley, New York, **1985**.
[4] A. J. Bridgeman, G. Cavigliasso, L. R. Ireland, J. Rothery, *J. Chem. Soc. Dalton Trans.* **2001**, 2095.
[5] A. J. Bridgeman, G. Cavigliasso, *J. Phys. Chem. A* **2003**, *107*, 4568.
[6] A. J. Bridgeman, G. Cavigliasso, *Faraday Discuss.* **2003**, *124*, 239.
[7] I. Mayer, *Chem. Phys. Lett.* **1983**, *97*, 270; I. Mayer, *Int. J. Quantum Chem.* **1984**, *26*, 151.
[8] K. A. Wiberg, *Tetrahedron* **1968**, *24*, 1083.
[9] R. A. Evarestov, V. A. Veryazov, *Theor. Chim. Acta* **1991**, *81*, 95.
[10] G. te Velde, F. M. Bickelhaupt, E. J. Baerends, G. Fonseca Guerra, T. Ziegler, *J. Comput. Chem.* **2001**, *22*, 931.
[11] C. E. Schäffer, *Struct. Bonding* **1973**, *14*, 69.
[12] A. J. Bridgeman, M. Gerloch, *Prog. Inorg. Chem.* **1997**, *45*, 179.
[13] ADF2000.02; E. J. Baerends, D. E. Ellis, P. Ros, *Chem. Phys.* **1973**, *2*, 41; L. Versluis, T. Ziegler, *J. Chem. Phys.* **1988**, *88*, 322; G. te Velde, E. J. Baerends, *J. Comput. Phys.* **1992**, *99*, 84; C. Fonseca Guerra, J. G. Snijders, G. te Velde, E. J. Baerends, *Theor. Chem. Acc.* **1998**, *99*, 391.
[14] J. C. Slater, *Phys. Rev.* **1930**, *36*, 57.
[15] E. van Lenthe, A. E. Ehlers, E. J. Baerends, *J. Chem. Phys.* **1999**, *110*, 8943.
[16] S. H. Vosko, L. Wilk, M. Nusair, *Can. J. Phys.* **1980**, *58*, 1200.
[17] W. Kohn, L. J. Sham, *Phys. Rev.* **1965**, *140*, A1133.
[18] A. D. Becke, *Phys. Rev. A* **1988**, *38*, 3098.
[19] J. P. Perdew, *Phys. Rev. B* **1986**, *33*, 8822.
[20] A. J. Bridgeman, C. J. Empson, *MAYER*, The University of Hull, Hull, U.K., 2005. Freely available on the worldwide web from http://www.hull.ac.uk/php/chsajb/mayer/.
[21] G. A. Landrum, N. Goldberg, R. Hoffman, *J. Chem. Soc. Dalton Trans.* **1997**, 3605.
[22] F. M. Bickelhaupt, E. J. Baerends, *Rev. Comput. Chem.* **2000**, *15*, 1.
[23] V. M. Rayón, G. Frenking, *Chem. Eur. J.* **2002**, *8*, 4693.
[24] A. J. Bridgeman, *J. Chem. Soc. Dalton Trans.* **1997**, 2887.
[25] W. Bunder, E. Weiss, *J. Organomet. Chem.* **1975**, *92*, 1.
[26] P. Seiler, J. D. Dunitz, *Acta. Crystallog. Sect B* **1979**, *35*, 1068.
[27] E. Gard, A. Haaland, D. P. Povak, R. Seip, *J. Organomet. Chem.* **1975**, *88*, 181.
[28] K. A. Lyssenko M. Y. Antipin, S. Y. Ketkov, *Russ. Chem. Bull.* **2001**, *50*, 130.
[29] M. Herberhold, T. Hofmann, W. Milius, B. Wrackmeyer, *J. Organomet. Chem.* **1994**, *472*, 175.
[30] P. E. Riley, *J. Organomet. Chem.* **1976**, *113*, 157.

Received: July 28, 2005
Published online: December 27, 2005

